How to cite: *Angew. Chem. Int. Ed.* **2023**, *62*, e202305817
doi.org/10.1002/anie.202305817

Photoactive Carbon Dots

Simultaneous Hydrogen Generation and Exciplex Stimulated Emission in Photobasic Carbon Dots

Jiawen Fang, Yiou Wang, Mariam Kurashvili, Sebastian Rieger, Wiktor Kasprzyk, Qingli Wang, Jacek K. Stolarczyk,* Jochen Feldmann, and Tushar Debnath**

Abstract: Photocatalytic water splitting is a promising approach to generating sustainable hydrogen. However, the transport of photoelectrons to the catalyst sites, usually within ps-to-ns timescales, is much faster than proton delivery (~ μs), which limits the activity. Therefore, the acceleration of abstraction of protons from water molecules towards the catalytic sites to keep up with the electron transfer rate can significantly promote hydrogen production. The photobasic effect that is the increase in proton affinity upon excitation offers means to achieve this objective. Herein, we design photobasic carbon dots and identify that internal pyridinic N sites are intrinsically photobasic. This is supported by steady-state and ultrafast spectroscopic measurements that demonstrate proton abstraction within a few picoseconds of excitation. Furthermore, we show that in water, they form a unique four-level lasing scheme with optical gain and stimulated emission. The latter competes with photocatalysis, revealing a rather unique mechanism for efficiency loss, such that the stimulated emission can act as a toggle for photocatalytic activity. This provides additional means of controlling the photocatalytic process and helps the rational design of photocatalytic materials.

Introduction

Efficient photocatalytic hydrogen production requires the concurrent transfer of protons and photoinduced electrons to the active sites on the surface of the catalysts.[1] However, there exists a substantial mismatch between the delivery time of protons and charge carriers. In general, the timescale of charge carrier generation, separation, and transfer range from subpicosecond to several nanoseconds.[2] Meanwhile, the timescale around 10–900 microseconds has been reported for hydrogen evolution,[3] wherein the proton transfer is the putative rate-determining step.[1] Therefore, a formidable challenge in photocatalysis is to ensure just-in-time delivery of both participants at the reaction sites. This can be achieved by increasing the electron lifetime or providing the protons sufficiently quickly. Several approaches have been explored to extend the lifetime of electrons, for instance the charge separation across a formation of heterojunction and the use of hole scavengers.[4] While earlier reports investigate the mechanism of charge carrier transfer/separation between carefully-tailored carbon dots (CDs) and graphitic carbon nitride (g-C_3N_4) for photocatalytic performance[5–7] we aim to directly tackle the issues of timescale mismatch in photocatalysis by accelerating the proton transfer via the fundamental understanding of photobase effect mechanism. Generally, hole scavengers are added to perform surrogate reactions involving sacrificial agents on the slow oxidation half-reaction to reduce the detrimental charge recombination, however, proton delivery is part of the reduction half-reaction. Recently, the acceleration of the proton transfer rate has been investigated utilizing the photobasic effect. In general, it depends on the

[*] Dr. J. Fang, Prof. Dr. Y. Wang, M. Kurashvili, Dr. S. Rieger, Dr. W. Kasprzyk, Prof. Dr. J. K. Stolarczyk, Prof. Dr. J. Feldmann, Dr. T. Debnath
Chair for Photonics and Optoelectronics, Department of Physics, Nano-Institute Munich, Ludwig-Maximilians-Universität München
Königinstr. 10, 80539 Munich (Germany)

Prof. Dr. Y. Wang, Q. Wang
Advanced Research Institute for Multidisciplinary Sciences, MOE Key Laboratory of Cluster Science & School of Chemistry and Chemical Engineering, Beijing Institute of Technology
No. 5 South Zhongguancun Street, Haidian District, Beijing, 100081 (China)
E-mail: yiou.wang@bit.edu.cn

Dr. W. Kasprzyk
Department of Biotechnology and Physical Chemistry, Faculty of Chemical Engineering and Technology, Cracow University of Technology
Warszawska 24, 31-155 Kraków (Poland)

Prof. Dr. J. K. Stolarczyk
Smoluchowski Institute of Physics, Faculty of Physics, Astronomy and Applied Computer Science, Jagiellonian University
Lojasiewicza 11, 30-348 Krakow (Poland)
E-mail: jacek.stolarczyk@uj.edu.pl

Dr. T. Debnath
Centre for Nanotechnology, Indian Institute of Technology Guwahati
Guwahati, Assam-781039 (India)
E-mail: t.debnath@iitg.ac.in

difference in the pKa at the ground state and excited state. The larger pKa confers the structure with a higher affinity to protons. This effect is typically associated with pyridinic heterocyclic moieties in the organic structures.[8] To this end, we have reported that a model photobasic molecule, acridine, can abstract a proton from water within 30 ps and can contribute to the photocatalytic H_2 generation of carbon nanomaterials.[1] Such a phenomenon draws attention to the role of photobasic moieties, specifically to nitrogen species in carbon nitrides and other nitrogen-containing polymeric photocatalysts in the mechanism of hydrogen production.[9]

Carbon-dots (CDs), composed of polyaromatic hydrocarbons with various functional groups, are promising candidates in applications such as (photo)catalysis, blue OLEDs, and sensing due to their unique electronic structures, ease of fabrication, photostability, and facile tunability.[10] In photocatalysis, CDs have been shown capable of performing several functions, e.g. as a sensitizer, a co-catalyst in peroxide decomposition and charge carrier acceptor or even a full photocatalyst for water splitting and CO_2 conversion.[11,12] Nitrogen doping has been reported as an effective approach to tune the properties of CDs. For example, the photoluminescence quantum yield (PLQY) of CDs can be considerably enhanced by introducing primary amines in the precursor.[13] Moreover, we have previously shown that the N-doped CDs behave in a trade-off manner regarding luminescent and photocatalytic properties.[14] The similarity of pyridynic nitrogen position in the CDs and in many photobasic molecules (e.g. acridine), suggests that CDs are themselves photobasic. This intrinsic photobasicity could contribute to their photocatalytic activity by enabling faster proton transfer to the reaction sites. However, direct evidence of such a hypothesis has not yet been reported. In effect, the limitations in photophysical understandings of the catalytic processes and how these different nitrogen moieties affect these processes hinder the rational design for improved photocatalytic performance.

Herein, we design and synthesize photobasic CDs (see Figure 1). We use steady-state and ultrafast transient absorption spectroscopy and find that CDs with pyridinic nitrogen display intrinsic photobasic functionality. Notably, we show that photobasic CDs can abstract protons from water within a few picoseconds after being excited. The ultrafast proton transfer in pyridinic N-containing CDs then promotes the photocatalytic hydrogen production process. Interestingly, the protonated CDs in the form of an exciplex with a unique four-level energy diagram show a net optical gain, leading to stimulated emission, and could be potentially developed for amplified stimulated emission purposes that can potentially control and switch on/off the photocatalytic reaction.

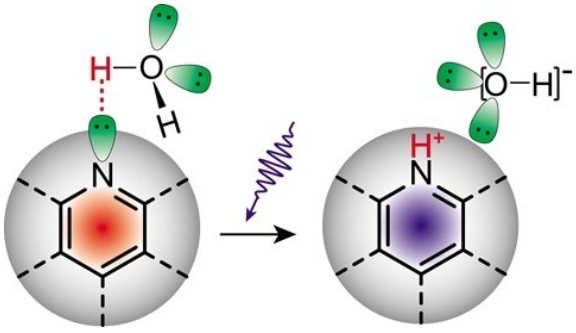

Figure 1. Schematic illustration of the photobasic effect of N-containing CDs.

Results and Discussion

Synthesis and Characterization

We prepared CDs with a well-documented hydrothermal method using citric acid and urea as precursors.[10e] Post-reaction, the residual reactants and existing small-molecular fluorophores were removed by a 24 h of dialysis, as illustrated in Figure 2a. The detailed preparation and treatment procedures are described in detail in the Supporting Information. The nitrogen amount in the final products was controlled by varying the ratio between citric acid and urea precursors. The samples were denoted as CD-1, CD-2, and CD-3 with an increasing molar ratio of urea to citric acid of 2:5, 5:2 and 11:1, respectively (see Supporting Information for details). The CD samples were initially characterized by high-resolution transmission electron microscopy (HRTEM) and X-ray diffraction (XRD) measurements. Monodisperse CDs were formed with average size ~23 nm for CD-3 sample, as can be seen from the TEM images in Figure 2b. Figure 2c shows HRTEM image of one single CD-3 particle, indicating an amorphous structure of the synthesized CDs. The XRD spectra of obtained CDs are shown in Figure S1. In all cases, the observed broad bands around $2\theta = 23.8°$ (3.74 Å) and 43° (2.11 Å) are far from a graphite-like pattern (usually at 26.5, 3.36 Å) and may be assigned to the (002) and (100) diffraction modes of an amorphous carbonaceous structure of CDs, respectively.[15]

We then performed X-ray photoelectron spectroscopy (XPS) to elucidate both, the chemical composition of obtained materials, and the effect of varying precursor concentration upon the chemical states of the elements in CDs (Figure 2d,e and Figure S2,S3). Firstly, survey spectra indicate that with an increasing ratio of urea to citric acid used for the synthesis, the sum of nitrogen and carbon species in CDs builds up at the expense of oxygen chemical states (see Figure S2). The high-resolution XPS analyses of C1s spectra for all samples exhibit three prominent peaks around 288.0 eV, 286 eV, and 284.8 eV, which corresponds to C=O, C–N/C–O, and C–H/C–C/C=C, respectively.[9a] In addition, there is an additional peak around 289.7 eV for CD-1, which can be attributed to carbon atoms in carboxylic, amide and/or anhydride groups. This peak was not present in CD-2 and CD-3 and is attributed to the residual citric acid that could not be reacted due to the lack of urea. In fact, O1s and N1s XPS spectra of CD-2 and CD-3 also lack the corresponding groups, supporting the assignment. Accordingly, the high-resolution O1s spectra of all samples indicate the presence of oxygen species typical for CDs

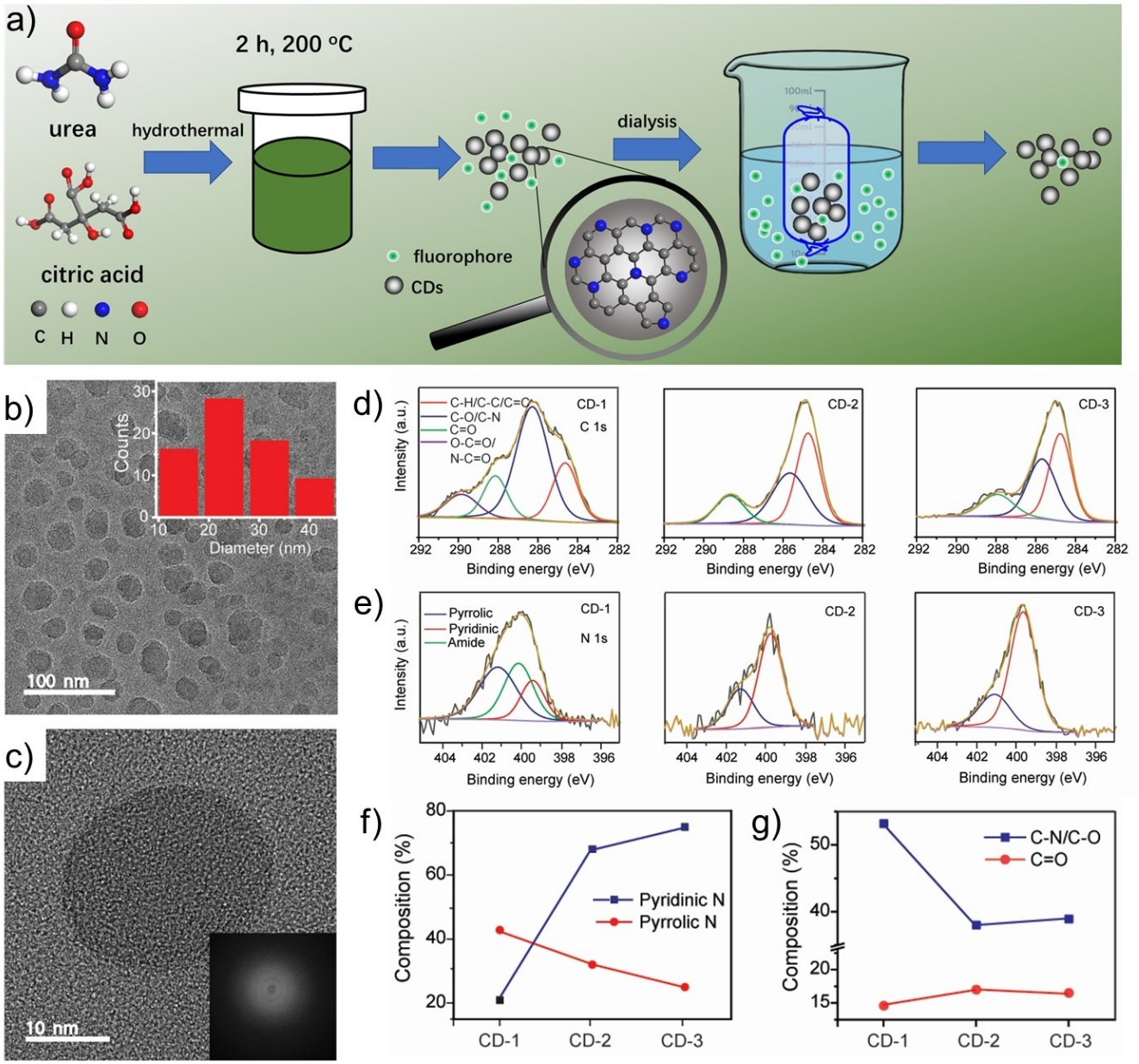

Figure 2. a) Schematic illustration of the synthesis procedure of photobasic CDs. b) TEM and c) HRTEM images of CD-3 sample. Inset in b) shows the size distribution pattern, while in c) selected area diffraction (SEAD) pattern of the CD-3 sample is shown. De-convoluted high-resolution XPS spectra of d) carbon (C 1s) and e) nitrogen (N 1s) for three different CDs of varying urea amount. f, g) Percentage composition of pyridinic and pyrrolic nitrogen, and C–N/C–O, C=O, for three different CDs under investigation.

(C–O and C=O), while additional carboxylic anhydride components were found only in CD-1 samples (common for CDs in which citric acid is the main precursor) (Figure S3).[16] The high-resolution N1s spectra centered around 399, 400 and 401 eV are assigned to pyridinic, amide and pyrrolic nitrogen structures, respectively.[14,17] From CD-1 to CD-3, the content of pyridinic N rises while that of pyrrolic N goes down (Figure 2f), indicating that a higher ratio of urea would result in more pyridinic N sites. The compositions of other functional moieties are summarized in Figure 2g and Table S1. As reported previously, the photobasic effect of acridine is related to the pyridinic N atom in the conjugated heterocyclic molecule, where the photoinduced protonation occurs.[18] The above result suggests the photobasic sites could be also formed in the prepared CD samples, offering the possibility of obtaining photobasic CDs.

We further performed Fourier transform infrared spectroscopy (FT-IR) of CD-3 samples (Figure S4). Firstly, as no clear bands associated with stretching modes of C=O of carboxylic acid show up around 1700–1760 cm^{-1} region, the presence of free carboxyl groups from citric acid have been ruled out, indicating complete conversion of this precursor during synthesis. The C=O units within CD structure exists most likely in the form of pyridones and/or amides (C=O

stretching bands around 1660 cm^{-1}). The broad band in 3400–2500 cm^{-1} regime was ascribed to overlapped stretching vibrations of C=C–H, C–C–H, O–H and N–H, while the band in 1500–1250 cm^{-1} region were attributed to C–O stretching and C–H bending vibrations.[19] In the low wavenumber region of the spectrum (<1000 cm^{-1}), two out-of-plane bending modes were observed: narrow band at 767 cm^{-1} (C–H in aromatics/heteroaromatics) and a broad N–H band of amines or amides (900–500 cm^{-1}). All the above results suggest the existence of a variety of functional groups within the sample which corresponds well to the typical picture of the CD structure. These results indicate that CD-3 with the highest concentration of pyridinic nitrogen atoms may possess the strongest photobasic properties. Therefore, we further investigated the CD-3 sample by optical spectroscopy to confirm the photobasic effect.

Optical Characterization

To identify whether CDs can abstract protons from water upon photoexcitation, we removed the aqueous solution, and re-dispersed CDs in an aprotic solvent, acetonitrile. Afterwards, a varying amount of water was added. According to the definition of the photobase effect, the photo-induced protonation occurs in the excited state. In effect, the absorption process should be independent of water content but the de-excitation (e.g. via luminescence) depends. To this end, we acquired UV/Vis absorption, PL and PL excitation (PLE) spectra to investigate the optical properties of CD-3. The resulting absorption spectra of the CDs dispersed in mixtures that had different ratios of water/acetonitrile (H_2O/CH_3CN, volume ratio) are shown in Figure 3a (additional data in Supporting Information, Figure S5). As expected, the normalized absorption spectra remain unchanged upon the addition of water. In contrast, the PL spectra reveal a noteworthy red shift with increasing water content in the CDs (Figure 3b, also Figure S6). The PL spectrum in pure acetonitrile exhibits a broad PL emission in the region between 350–550 nm with a maximum at ~400 nm upon excitation at 330 nm. Upon the addition of an increasing amount of water as a proton source, starting with 0.5 %, the peak position is red-shifted. It reaches

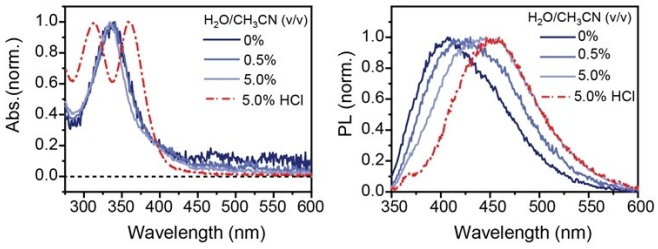

Figure 3. a) UV/Vis absorption spectra and b) photoluminescence (PL, $\lambda_{ex}=330$ nm) spectra of the CD-3 in different water/acetonitrile (H_2O/CH_3CN, v/v) mixture of varying water amount between 0% and 5%. The absorption and PL spectra in the presence of 5% HCl in the acetonitrile solution is also illustrated (red dot-dashed line) for comparison.

460 nm at 5 % water content. At the same time, the PLE spectra remain unaltered (Figure S7) implying a presence of protonated CDs in the excited state, consistent with the photobasic character. This suggests that the majority of PL at ~460 nm stems from the protonated CDs.

Additional evidence regarding the photobasic nature of the CD comes from absorption and PL experiments performed in the presence of 5 % HCl in acetonitrile solution. In this case, the CDs become protonated even in the ground state, as shown in the corresponding absorption spectrum (Figure 3a and Figure S5b). The protonated CDs emit at ~460 nm, as shown in Figure 3b. The PL spectrum of the 5 % water/acetonitrile mixture appears remarkably similar to that of 5 % HCl/acetonitrile solution in the red region of the spectra (Figure 3b), indicating a substantial part of the CDs is indeed protonated in the excited state in 5 % water/acetonitrile mixture. In conclusion, the appearance of nearly identical absorption spectra together with a red-shift of the PL spectra with an increasing amount of water indicate the photobasic character of the CDs.

Protonation Dynamics

After establishing the photobasic character of the CDs, we turn our attention to estimating the rate of proton transfer in the excited state of such CDs. To this end, we performed femtosecond transient absorption (TA) spectroscopic measurements of the CDs dispersed in pure acetonitrile, pure water, and acetonitrile/water mixtures. We excited the CDs at 330 nm with a ~100 fs pump pulse and acquired the differential absorption spectra with a time-delayed white light probe pulse. The TA spectrum of the CDs in the pure acetonitrile solution consists of a broad and structureless excited state absorption (ESA) in the entire probe region, between 350–700 nm (Figure 4a, b). Previously, the broad ESA has been attributed to the transient absorption to higher excited states caused by the photoexcited carriers (see further details in the SI).[20,21] Upon the addition of 10 % of water (see Figures 4c, d) to the acetonitrile solution, the TA spectrum of the CDs changes significantly for longer delay times. At very early times (<200 fs), the TA spectrum still looks similar to the pure acetonitrile solution, consisting of the broad ESA. However, at later times, a strong negative ΔA signal emerges between 400 to 550 nm on top of the ESA signal.

The absorption spectrum of the CDs has a maximum at 340 nm, with a very low absorption cross-section above 400 nm, irrespective of the amount of water in acetonitrile (Figure 3a). Therefore, the negative ΔA signal in this transparent region cannot be attributed to the ground state bleach. Instead, it is attributed to the stimulated emission (SE) from the photoexcited CDs. To verify this argument, the TA spectra is compared with the PL spectrum of the CDs in the same solvent mixture with the reversed sign. The clear overlap in the range between 400 to 550 nm of the PL with the negative ΔA signal corroborates the assignment to SE (Figure 4d). In particular, the early time (<1 ps) negative ΔA signal has significant overlap with the high-

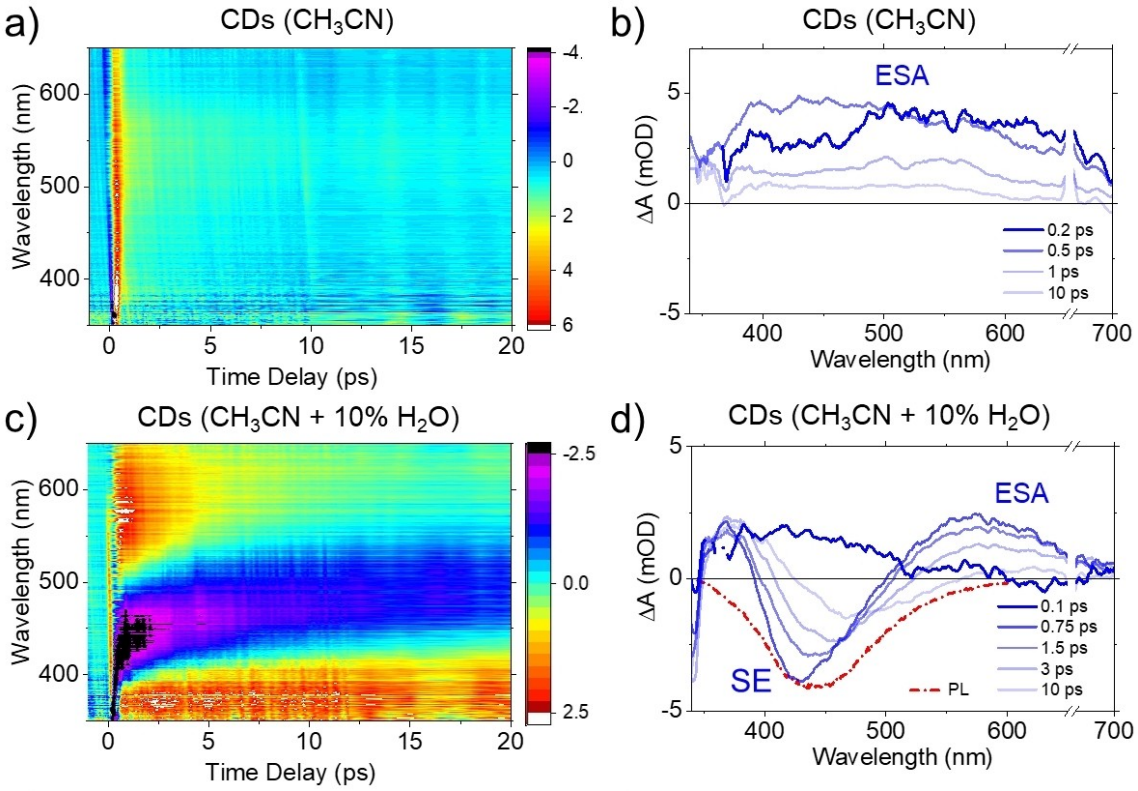

Figure 4. Transient absorption spectra of CD-3 after excitation at 330 nm a, b) in pure acetonitrile (CH_3CN) and c, d) in the presence of 10% water in acetonitrile solution in a contour diagram and at the selected time delays between 0.1 to 10 ps, respectively. The PL spectrum (inverted) is also plotted in a red dot-dashed line in panel d). Note the break in the x-axis between 650 and 660 nm in panels b) and d) to remove the contribution from the second harmonic of the 330 nm pump pulse. For clear presentation, the spectra in b) and d) are smoothened.

energy side of the PL while it has more overlap with the lower energy side of the PL at a later time (~10 ps). Further evidence of the SE comes when the early time (~0.5 ps) TA spectrum of the CDs in pure acetonitrile is subtracted from the TA spectrum acquired for 10% water content. This 'difference spectrum' is then compared with the corresponding PL spectrum, with the two spectra almost sitting on top of each other (Figure 5a and Figure S8). We also performed analogous experiments in pure water where CDs have easier access to protons and observe a similar but stronger SE signal on top of the ESA signal, as shown in Figure S9. The 'difference spectrum' obtained by subtraction of the TA spectrum of the CDs in pure water and pure acetonitrile solution overlaps nicely with the PL spectrum in pure water (Figure S10), albeit at an earlier time (~0.3 ps) than in the 10% water/acetonitrile mixture.

The origin of SE is schematically depicted in Figure 5b. In the presence of water, the CDs attract a proton from the water molecule in the excited state due to its photobasic property and form the corresponding exciplex species (i.e. the protonated CD, $B^*–H^+$). By emitting a low-energy photon, the exciplex then relaxes to produce the complex in the ground state. As the protonated ground state ($B–H^+$) is energetically higher than the non-protonated ground state (B), a rapid relaxation from $B–H^+$ to B takes place corresponding to the de-protonation process. Therefore, a population inversion can be achieved in the exciplex state ($B^*–H^+$) with respect to the protonated ground state ($B–H^+$) and appears as the SE in the TA spectra. The observation of the SE feature from an exciplex state in nitrogen-derived CDs is unique and can be understood in terms of a four-level system of the exciplex, as shown in Figure 5b.

We further estimated the proton transfer time by inspecting the time it takes the SE signal to appear. As there is a strong overlap between the SE and the ESA signals, to shift away from the ESA feature, we plot the TA transients at 490 nm (Figure 5c) where the contribution due to the ESA is minimal, in both 10% water/acetonitrile mixture and pure water. The transient in a pure acetonitrile solution at 490 nm consists of ultrafast (~200 fs) and 4 ps decay components. For both the 10% water/acetonitrile and pure water sample, initially, an ESA feature is observed, which decays with ~250 fs, similar to the fast component in pure acetonitrile solution. The onset growth time of the SE signal can be characterized by 2.1 ps and 1.7 ps for 10% water/acetonitrile and pure water, respectively. Here the growth in the SE signal must correspond to the proton transfer time in the excited state. The faster protonation time in the presence of pure water (1.7 ps) compared to a 10% water/acetonitrile mixture (2.1 ps) is also consistent with the increased availability of protons. It is important to note that

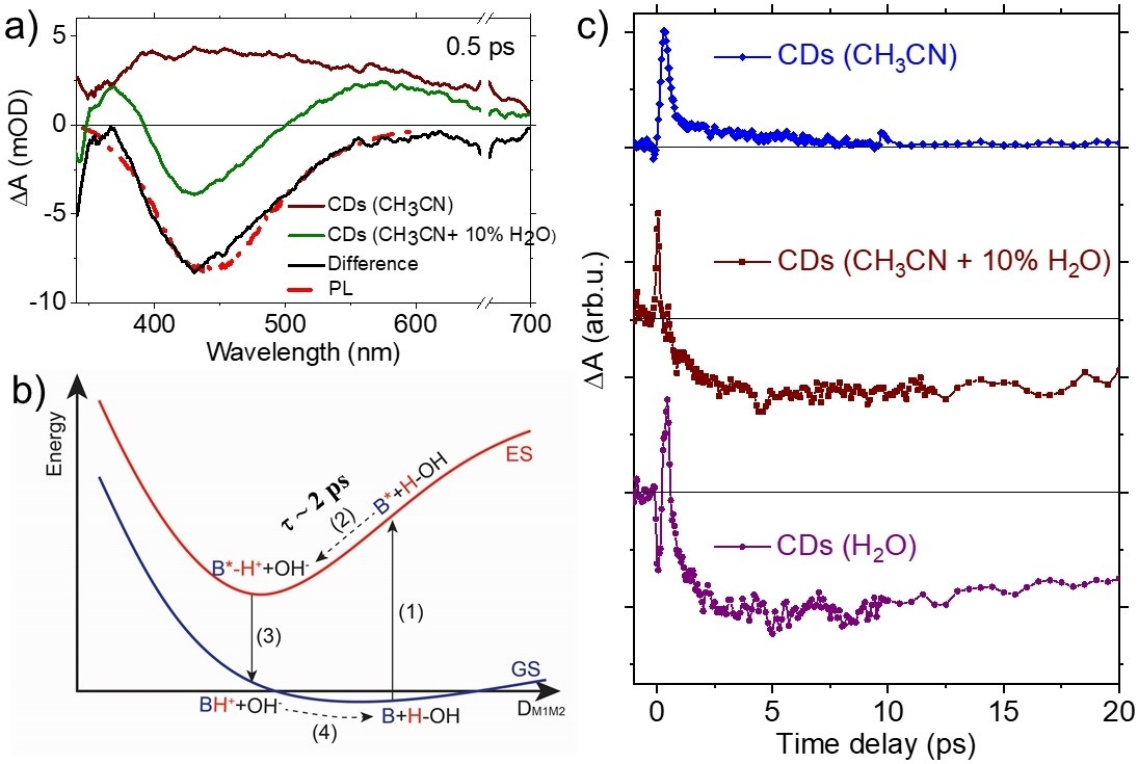

Figure 5. a) The early time (~0.5 ps) TA spectra of CD-3 in pure acetonitrile and 10% water/acetonitrile mixture solution, along with the difference between the two (in black line), are shown. The PL spectrum (inverted) is also plotted in a red dot-dashed line for comparison. b) Schematic illustration of the exciplex formation in the CDs, driven by the photobasic CDs. In the first step, photoexcitation of the CDs (shown as B) leads to the formation of the excited CDs (B*), which then abstract a proton from the neighboring water molecule in the second step owing to the increased proton affinity. The protonated CDs (B*–H^+) relax via lower energy photon emission to produce the ground state protonated species (B–H^+) in the third step. Finally, the dissociation of the proton regenerates the CDs in the ground state in the fourth step. c) Comparison of the transient traces of the CDs at 490 nm in pure acetonitrile, 10% water in acetonitrile and pure water solution.

the excited state protonation time in the present work is an order of magnitude faster as compared to our previous report (~30 ps), where we used an extrinsic photobasic molecule to sensitize the CDs. We speculate the presence of multiple photobasic sites in the CDs (as can be inferred from Figure 2e), along with electron donors (e.g. $–NH_2$, –OH, etc.) that accelerate the excited protonation process more than the reported acridine molecule, containing a single photobasic site.[18] Hydrogen generation could involve two such photobasic sites in the vicinity which then proceed via Tafel step to produce an H_2 molecule. Alternatively, the process may involve another water molecule (or proton) at the same site, in the Heyrovsky step to generate an H_2 molecule. Such very fast, only several picoseconds, timescale of the process suggests that the proton abstraction does not involve proton diffusion, but rather occurs from a nearby, complexed water molecule. As proton delivery is thought to be one of the main (if not the main) limiting steps in photocatalysis reaction, this method can significantly enhance the reduction rate of protons and hydrogen generation, as discussed in the next section.

Photocatalysis

To understand how the N-species in photobasic CDs influence the proton reduction activity, we evaluated the hydrogen evolution rate (HER) on three different CDs with varying amounts of nitrogen doping under the irradiation of a solar simulator coupled with an IR filter. To focus on the nitrogen-containing moieties, no platinum co-catalysts were added. Negligible hydrogen was produced on CD-1 at neutral pH. Without enough photobasic nitrogen sites to extract protons, CD-1 shows no activity. However, when the pyridinic N content increases, the HER of CD-2 reached 6.5 $\mu mol\,g^{-1}h^{-1}$ and further to 12.12 $\mu mol\,g^{-1}h^{-1}$ on CD-3 (Figure 6a and Figure S12). As the number of pyridinic N sites increase in CDs, an enhancement of proton becomes relevant. This dramatic improvement in the HER with different amounts of nitrogen doping agrees with our prediction based on optical measurements. Figure 6a reveals that the photocatalytic hydrogen production in the first hour is slower compared to a later time. This is possibly due to delayed activation of the CDs by the initial photoinduced reactions on the CD surface and can be attributed to removal of the passivating layer, oxidation of pendant groups or scraping of amorphous phase. In addition, initially hydrogen may form as hydrogen atoms adsorbed on the CD

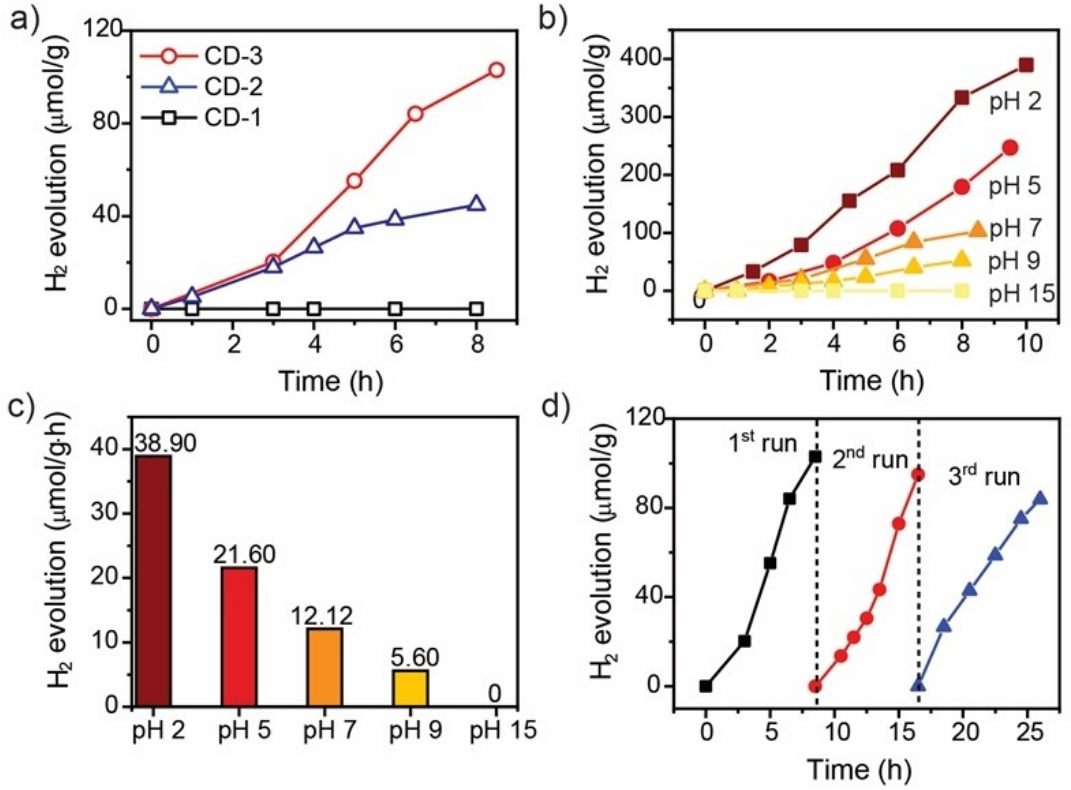

Figure 6. a) Photocatalytic H_2 production formation rate of three different CDs. The photocatalytic performance of CD-3 sample at different pH (2, 5, 7, 9, 15) for b) hydrogen production and c) the average rate of hydrogen production. d) Long-term photocatalytic H_2 production formation rate of CD-3 sample for three different runs.

surface (i.e. Volmer step) and only in the second step H_2 molecules are formed.

In order to further investigate how the photobase effect influences the kinetics under neutral to acidic or basic concentrations of protons, we measured the HER for a range of pH values between 2 to 15 on CD-3. Under neutral pH, the CD sample exhibits a hydrogen evolution rate of 12.12 $\mu mol\,g^{-1}h^{-1}$ which reduces with increasing pH (Figure 6b,c). For example, negligible hydrogen is detected under highly basic conditions (pH = 15), where the photobasic protonation process is suppressed. Easier access to proton at pH 7 than at pH 9 or pH 15 results in a higher HER activity at pH 7. In contrast, at acidic pH the hydrogen evolution increases drastically with a rate as high as ~39 $\mu mol\,g^{-1}h^{-1}$, with enhancement in the apparent quantum yield (see SI). Moreover, we performed repeated long-term photocatalytic H_2 production experiments which showed relatively high formation rate for three different cycles, indicating promising durability of the CD-3 catalyst (Figure 6d). It should be noted that such phenomenon differs from those on some N-free inorganic systems in the literature, including our previous Ni-decorated CdS, where strong alkaline conditions were reported to prolong the lifetime of photogenerated electrons by quickly eliminating the holes with OH^- to form hydroxyl radicals.[22] However, such systems usually need efficient co-catalysts such as Pt and Ni to accept electrons from photocatalysts and extract protons from water even at a low concentration. In the present study, we show that intrinsically photobasic CDs could attract protons without the need for additional co-catalysts, although such a photobase effect only works at a certain range of pH.

It should be noted that the simulated emission in the four-level electronic diagram is competing with photocatalysis (Figure 7), considering the fate of the exciplex species. In other words, a higher intensity of photon flux can accelerate charge recombination via stimulated emission and decrease the quantum efficiency of photocatalytic hydrogen production. Such a model derived from this study could explain the observation of the negligible effect of photocatalytic activity upon increasing light intensity from 75 mW/cm^2 to 150 mW/cm^2 by Yang et al.[23] Since there are pyridinic N species in the carbon nitride (heptazine) framework, the simulated emission discussed in this study could also be a reason for such a decline in its performance.

Photocatalysis at the surface of CDs is a complex process which may also involve unwanted side reactions, decreasing the selectivity of the desired reaction. The observations reported here of a four-level system open an exciting opportunity to block unwanted photocatalytic pathways by stimulating the emission from the excited protonated species. In this way, a competing SE process is promoted at the expense of the reaction that leads to an undesired product.

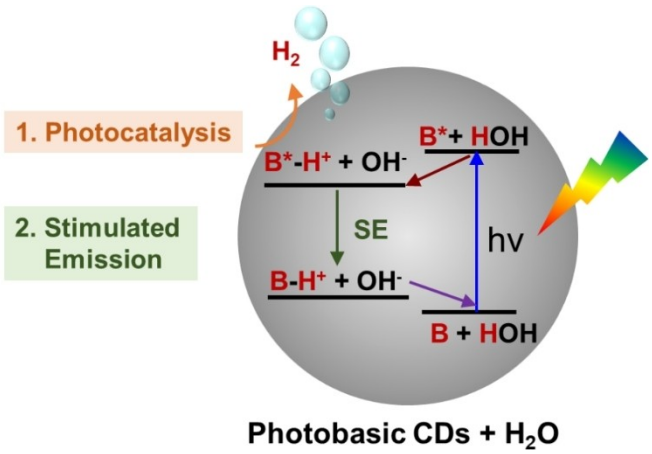

Figure 7. Photobasic CDs in a polar-protic environment upon photoexcitation demonstrate two contrasting phenomena: in the first case, the photoexcited electron driven by the existence of a local energy minimum of the protonated species ($B^*–H^+$) can emit back to the empty ground state of the protonated CDs ($B–H^+$), leading to exciplex SE behavior. In the second case, the photoexcited electron, rather than going back to the ground state, can reduce the H^+ (from the $B^*–H^+$) to produce H_2.

Conclusion

In summary, using ultrafast spectroscopy, we have shown that the N-containing pyridinic CDs are intrinsically photobasic, which can abstract a proton from water at the excited state within a few picoseconds, much faster than our previous report of a CDs decorated with a model photobase molecule. Our results demonstrate such ultrafast proton transfer significantly promotes the overall photocatalytic hydrogen production process. This is consistent with observations that pyridinic N sites likely account for the high photocatalytic H_2 production in these organic photocatalysts containing electron-withdrawing groups, such as carbon nitride materials,[24] and covalent triazine frameworks.[25] Such an ultrafast protonation process in CDs that are intrinsically photobasic can have potential applications not only in photocatalysis but also in opto-protonics, e.g. exciplex lasing. The unique electronic structure of such photobasic CDs shows a four-level exciplex diagram, which leads to optical gain in the excited state and could be further developed for lasing purposes. We believe that the present demonstration of carbon dots could stimulate the rational design of organic photocatalysts and lead to further enhancements in catalytic activity and light emission.

Acknowledgements

We acknowledge financial support from the Bavarian State Ministry of Science and Arts and by the LMU Munich through the grant "Solar Technologies go Hybrid (SolTech), the China Scholarship Council (J. F.), the Alexander von Humboldt Foundation (T.D. and Y.W.) and by the Strategic Program Excellence Initiative at the Jagiellonian University 'SciMat' (Grant U1U/W17/NO/01.04) (J.K.S.). We thank local research clusters and centers such as the Center of Nanoscience (CeNS) and e-conversion for providing communicative networking structures. T.D. acknowledges the Department of Science & Technology (DST) and the Science and Engineering Research Board (SERB) of India for the Ramanujan Fellowship Award (RJF/2021/000125). Y. W. thanks Teli Young Scholar Fellowship, National Natural Science Foundation of China for financial support (52203349) and Dr. Tongtong Gao for the assistance in HRTEM measurement. W.K. acknowledges the Polish National Agency for Academic Exchange for The Bekker Programme scholarship (PPN/BEK/2018/1/00460/U/00001). Open Access funding enabled and organized by Projekt DEAL.

Conflict of Interest

The authors declare no conflict of interest.

Data Availability Statement

The data that support the findings of this study are available from the corresponding author upon reasonable request.

Keywords: Excited State Proton Transfer · Photobasic Carbon Dots · Photocatalytic Hydrogen Generation · Stimulated Emission · Ultrafast Timescale

[1] J. Tang, J. R. Durrant, D. R. Klug, *J. Am. Chem. Soc.* **2008**, *130*, 13885–13891.
[2] J. K. Stolarczyk, S. Bhattacharyya, L. Polavarapu, J. Feldmann, *ACS Catal.* **2018**, *8*, 3602–3635.
[3] A. Yamakata, T.-a. Ishibashi, H. Onishi, *J. Phys. Chem. B* **2001**, *105*, 7258–7262.
[4] a) Q. Wang, S. Kalathil, C. Pornrungroj, C. D. Sahm, E. Reisner, *Nat. Catal.* **2022**, *5*, 633–641; b) S. Song, H. Song, L. Li, S. Wang, W. Chu, K. Peng, X. Meng, Q. Wang, B. Deng, Q. Liu, Z. Wang, Y. Weng, H. Hu, H. Lin, T. Kako, J. Ye, *Nat. Catal.* **2021**, *4*, 1032–1042.
[5] a) D. Qu, J. Liu, X. Miao, M. Han, H. Zhang, Z. Cui, S. Sun, Z. Kang, H. Fan, Z. Sun, *Appl. Catal. B* **2018**, *227*, 418–424; b) S. Zhang, M. Gao, Y. Zhai, J. Wen, J. Yu, T. He, Z. Kang, S. Lu, *J. Colloid Interface Sci.* **2022**, *622*, 662–674.
[6] B. Jana, Y. Reva, T. Scharl, V. Strauss, A. Cadranel, D. M. Guldi, *J. Am. Chem. Soc.* **2021**, *143*, 20122–20132.
[7] a) B. Li, W. Peng, J. Zhang, J.-C. Lian, T. Huang, N. Cheng, Z. Luo, W.-Q. Huang, W. Hu, A. Pan, L. Jiang, G.-F. Huang, *Adv. Funct. Mater.* **2021**, *31*, 2100816; b) B. Li, Z. Tian, L. Li, Y.-H. Wang, Y. Si, H. Wan, J. Shi, G.-F. Huang, W. Hu, A. Pan, W.-Q. Huang, *ACS Nano* **2023**, *17*, 3465–3482.
[8] a) M. Noboru, K. Yozo, K. Masao, *Bull. Chem. Soc. Jpn.* **1956**, *29*, 373–379; b) J. R. Hunt, J. M. Dawlaty, *J. Phys. Chem. A* **2018**, *122*, 7931–7940.
[9] a) Y. Wang, M. K. Bayazit, S. J. A. Moniz, Q. Ruan, C. C. Lau, N. Martsinovich, J. Tang, *Energy Environ. Sci.* **2017**, *10*, 1643–1651; b) Y. Wang, A. Vogel, M. Sachs, R. S. Sprick, L. Wilbraham, S. J. A. Moniz, R. Godin, M. A. Zwijnenburg, J. R. Durrant, A. I. Cooper, J. Tang, *Nat. Energy* **2019**, *4*, 746–760;

c) V. S. Vyas, F. Haase, L. Stegbauer, G. Savasci, F. Podjaski, C. Ochsenfeld, B. V. Lotsch, *Nat. Commun.* **2015**, *6*, 8508; d) K. Schwinghammer, B. Tuffy, M. B. Mesch, E. Wirnhier, C. Martineau, F. Taulelle, W. Schnick, J. Senker, B. V. Lotsch, *Angew. Chem. Int. Ed.* **2013**, *52*, 2435–2439; e) K. Schwinghammer, M. B. Mesch, V. Duppel, C. Ziegler, J. Senker, B. V. Lotsch, *J. Am. Chem. Soc.* **2014**, *136*, 1730–1733.

[10] a) F. Arcudi, L. Đorđević, M. Prato, *Acc. Chem. Res.* **2019**, *52*, 2070–2079; b) S. Y. Lim, W. Shen, Z. Gao, *Chem. Soc. Rev.* **2015**, *44*, 362–381; c) S. Zhu, Y. Song, X. Zhao, J. Shao, J. Zhang, B. Yang, *Nano Res.* **2015**, *8*, 355–381; d) M. Han, S. Zhu, S. Lu, Y. Song, T. Feng, S. Tao, J. Liu, B. Yang, *Nano Today* **2018**, *19*, 201–218; e) W. Kasprzyk, T. Świergosz, P. P. Romańczyk, J. Feldmann, J. K. Stolarczyk, *Nanoscale* **2022**, *14*, 14368–14384.

[11] a) G. A. M. Hutton, B. Reuillard, B. C. M. Martindale, C. A. Caputo, C. W. J. Lockwood, J. N. Butt, E. Reisner, *J. Am. Chem. Soc.* **2016**, *138*, 16722–16730; b) B. C. M. Martindale, G. A. M. Hutton, C. A. Caputo, E. Reisner, *J. Am. Chem. Soc.* **2015**, *137*, 6018–6025; c) L. Cao, S. Sahu, P. Anilkumar, C. E. Bunker, J. Xu, K. A. S. Fernando, P. Wang, E. A. Guliants, K. N. Tackett, Y.-P. Sun, *J. Am. Chem. Soc.* **2011**, *133*, 4754–4757; d) Y. Dong, H. Pang, H. B. Yang, C. Guo, J. Shao, Y. Chi, C. M. Li, T. Yu, *Angew. Chem. Int. Ed.* **2013**, *52*, 7800–7804; e) Y. Wang, X. Liu, X. Han, R. Godin, J. Chen, W. Zhou, C. Jiang, J. F. Thompson, K. B. Mustafa, S. A. Shevlin, J. R. Durrant, Z. Guo, J. Tang, *Nat. Commun.* **2020**, *11*, 2531; f) J. Liu, Y. Liu, N. Liu, Y. Han, X. Zhang, H. Huang, Y. Lifshitz, S.-T. Lee, J. Zhong, Z. Kang, *Science* **2015**, *347*, 970–974.

[12] T.-F. Yeh, C.-Y. Teng, S.-J. Chen, H. Teng, *Adv. Mater.* **2014**, *26*, 3297–3303.

[13] X. Zhai, P. Zhang, C. Liu, T. Bai, W. Li, L. Dai, W. Liu, *Chem. Commun.* **2012**, *48*, 7955–7957.

[14] S. Bhattacharyya, F. Ehrat, P. Urban, R. Teves, R. Wyrwich, M. Döblinger, J. Feldmann, A. S. Urban, J. K. Stolarczyk, *Nat. Commun.* **2017**, *8*, 1401.

[15] a) C. Hu, Y. Liu, Y. Yang, J. Cui, Z. Huang, Y. Wang, L. Yang, H. Wang, Y. Xiao, J. Rong, *J. Mater. Chem. B* **2013**, *1*, 39–42; b) L. Qu, Y. Liu, J.-B. Baek, L. Dai, *ACS Nano* **2010**, *4*, 1321–1326; c) Y. Li, L. Mu, Y.-S. Hu, H. Li, L. Chen, X. Huang, *Energy Storage Mater.* **2016**, *2*, 139–145.

[16] M. Ortega-Muñoz, P. Vargas-Navarro, F. Hernandez-Mateo, A. Salinas-Castillo, L. F. Capitan-Vallvey, S. Plesselova, R. Salto-Gonzalez, M. D. Giron-Gonzalez, F. J. Lopez-Jaramillo, F. Santoyo-Gonzalez, *Nanoscale* **2019**, *11*, 7850–7856.

[17] a) H. Wang, T. Maiyalagan, X. Wang, *ACS Catal.* **2012**, *2*, 781–794; b) J. D. Bagley, D. K. Kumar, K. A. See, N.-C. Yeh, *RSC Adv.* **2020**, *10*, 39562–39571.

[18] J. Fang, T. Debnath, S. Bhattacharyya, M. Döblinger, J. Feldmann, J. K. Stolarczyk, *Nat. Commun.* **2020**, *11*, 5179.

[19] Y. Wang, F. Silveri, M. K. Bayazit, Q. Ruan, Y. Li, J. Xie, C. R. A. Catlow, J. Tang, *Adv. Energy Mater.* **2018**, *8*, 1801084.

[20] a) L. Wang, S.-J. Zhu, H.-Y. Wang, Y.-F. Wang, Y.-W. Hao, J.-H. Zhang, Q.-D. Chen, Y.-L. Zhang, W. Han, B. Yang, H.-B. Sun, *Adv. Opt. Mater.* **2013**, *1*, 264–271; b) J. P. Guin, S. K. Guin, T. Debnath, H. N. Ghosh, *Carbon* **2016**, *109*, 517–528; c) P. Jing, D. Han, D. Li, D. Zhou, L. Zhang, H. Zhang, D. Shen, S. Qu, *Adv. Opt. Mater.* **2017**, *5*, 1601049.

[21] a) L. Wang, H.-Y. Wang, Y. Wang, S.-J. Zhu, Y.-L. Zhang, J.-H. Zhang, Q.-D. Chen, W. Han, H.-L. Xu, B. Yang, H.-B. Sun, *Adv. Mater.* **2013**, *25*, 6539–6545; b) L. Sui, W. Jin, S. Li, D. Liu, Y. Jiang, A. Chen, H. Liu, Y. Shi, D. Ding, M. Jin, *Phys. Chem. Chem. Phys.* **2016**, *18*, 3838–3845.

[22] T. Simon, N. Bouchonville, M. J. Berr, A. Vaneski, A. Adrović, D. Volbers, R. Wyrwich, M. Döblinger, A. S. Susha, A. L. Rogach, F. Jäckel, J. K. Stolarczyk, J. Feldmann, *Nat. Mater.* **2014**, *13*, 1013–1018.

[23] W. Yang, R. Godin, H. Kasap, B. Moss, Y. Dong, S. A. J. Hillman, L. Steier, E. Reisner, J. R. Durrant, *J. Am. Chem. Soc.* **2019**, *141*, 11219–11229.

[24] a) X. Liang, S. Xue, C. Yang, X. Ye, Y. Wang, Q. Chen, W. Lin, Y. Hou, G. Zhang, M. Shalom, Z. Yu, X. Wang, *Angew. Chem. Int. Ed.* **2023**, *62*, e202216434; b) T. Jia, D. Meng, R. Duan, H. Ji, H. Sheng, C. Chen, J. Li, W. Song, J. Zhao, *Angew. Chem. Int. Ed.* **2023**, *62*, e202216511; c) J. Zhang, X. Liang, C. Zhang, L. Lin, W. Xing, Z. Yu, G. Zhang, X. Wang, *Angew. Chem. Int. Ed.* **2022**, *61*, e202210849; d) X. Fan, Z. Wang, T. Lin, D. Du, M. Xiao, P. Chen, S. A. Monny, H. Huang, M. Lyu, M. Lu, L. Wang, *Angew. Chem. Int. Ed.* **2022**, *61*, e202204407; e) X. Wang, K. Maeda, A. Thomas, K. Takanabe, G. Xin, J. M. Carlsson, K. Domen, M. Antonietti, *Nat. Mater.* **2009**, *8*, 76–80.

[25] a) V. Stavila, S. Li, C. Dun, M. A. T. Marple, H. E. Mason, J. L. Snider, J. E. Reynolds III, F. El Gabaly, J. D. Sugar, C. D. Spataru, X. Zhou, B. Dizdar, E. H. Majzoub, R. Chatterjee, J. Yano, H. Schlomberg, B. V. Lotsch, J. J. Urban, B. C. Wood, M. D. Allendorf, *Angew. Chem. Int. Ed.* **2021**, *60*, 25815–25824; b) W. Zhao, P. Yan, H. Yang, M. Bahri, A. M. James, H. Chen, L. Liu, B. Li, Z. Pang, R. Clowes, N. D. Browning, J. W. Ward, Y. Wu, A. I. Cooper, *Nat. Synth.* **2022**, *1*, 87–95; c) X. Hu, Z. Zhan, J. Zhang, I. Hussain, B. Tan, *Nat. Commun.* **2021**, *12*, 6596.

Manuscript received: April 26, 2023
Accepted manuscript online: June 22, 2023
Version of record online: July 10, 2023